Researchers Journal of Science and Technology (REJOST)
https://rejost.com.ng

Depth to basement estimation from aerogravity data over the Southeastern part of Niger Delta region of Nigeria

Aniekan E. Ekpo*[1], Nsikak E. Bassey[1], Nyakno J. George[2], Itoro G. Udo[1]

Received: July 3, 2024 /Accepted: September 5, 2024

© REJOST 2024

Abstract

This study presents a geological interpretation of aerogravity anomalies over the southeastern part of the Niger Delta Basin, Nigeria, with a focus on identifying subsurface structures related to hydrocarbon and mineral prospecting. High-resolution aerogravity data, collected by Fugro Airborne Surveys Canada between 2005 and 2010, were processed using Oasis Montaj (v7.0.1), Surfer (v16.6), and ArcGIS (v10.4) software. The study employed various data filtering and enhancement techniques, including Fast Fourier Transform (FFT) for spectral analysis, Euler deconvolution, and 2D forward modeling. The Butterworth filter, with a central wave number of 1900 and degree 2, was used to separate regional and residual anomalies. The regional gravity anomaly map exhibited a Bouguer gravity range from -7.3 mGal to 39.4 mGal, with prominent trends in NE-SW, N-S, and NW-SE directions, indicating deep-seated subsurface structures. The residual gravity map, filtered with a central wave number of 3 and degree 8, revealed structural features including linear, ellipsoidal, and irregular-shaped anomalies extending primarily in the N-S, NE-SW, and NW-SE directions. Euler deconvolution analysis showed depth ranges from a minimum of less than 34.4 m to a maximum of over 8,228 m, identifying subsurface fault structures aligned with the prevailing lineament patterns of the Niger Delta. Radial power spectrum analysis, applied to eight subdivided blocks of the study area, identified three depth ranges: shallow, intermediate, and deep sources. The 2D forward modeling using the GM-SYS package delineated the basement topography and subsurface structures across five key profiles, revealing undulating basement features with depths varying from approximately 6,000 m to over 10,000 m. Significant geological features were identified, including a major dyke intrusion along Profile 1 and domal uplift features along Profile 2, suggesting mantle plume activity. The results indicate a complex subsurface architecture characterized by variations in rock density and structural configurations, suggesting the presence of geological conditions favorable for hydrocarbon accumulation and mineral deposits. Regions with high-frequency anomalies, characterized by the concentration of short wavelength anomalies, such as the Oban Massif, are

associated with dense rock formations like granite, granodiorite, gneiss and migmatite and may contain valuable minerals and rare earth elements. The high-frequency anomalies around Ikot Ekpene, Aba, and Degema areas may be due to high density materials of lateral extent. Overall, the study demonstrates the effectiveness of using Bouguer gravity data in subsurface geological mapping and resource exploration. Blocks D1-D8 are recommended for further investigation for hydrocarbon exploration because they exhibit depths greater than 4000 m.

✉ Aniekan E. Ekpo: acdiamonmarkng@gmail.com

[1] Department of Geology, Akwa Ibom State University, Mkpat Enin, Akwa Ibom State, Nigeria

[2] Department of Physics, Akwa Ibom State University, Mkpat Enin, Akwa Ibom State, Nigeria

Keywords: Gravity method, hydrocarbon exploration, Mineral exploration, Niger Delta, Southeastern Nigeria

1.0 Introduction

Geophysics is the application of the laws of Physics to the study of rocks at the surface, shallow or at greater depths. Hence, as rocks differ according to their origin, structure, textures, etc., they also differ by their densities, magnetization, resistivity, and other physical parameters. Although most of the physical parameters of geophysics are non-unique, which is a principal problem of geophysics; it gives a clue on the possible geology of the subsurface at designated points. Geophysics has the advantage of being able to Image and delineate hidden structures and features inaccessible to direct observations and inspection, from measurements made on the surface of the earth either at a point, profile, and or grid.

Gravity anomaly arises from the density difference between a body of rocks and its surrounding host rocks. Density of rocks and their density contrasts control gravity anomalies which aids in identification of rocks, assessment of rock conditions and estimation of rock ore abundances (Amigun and Ako, 2009). The gravity method can be used at the early stages of exploration for petroleum as a reconnaissance tool. The advantage of this method of survey is its ability to cover a large span of area, most especially in areas with social, economic, political barriers, or environmentally hazardous zones (Murphy, 2007). Depending on the geologic setting and rock parameters of the area, one can use gravity data in various ways to solve different exploration problems (Ezekiel *et al*., 2013; Okiwelu *et al*., 2013; Obiora *et al*., 2016). The aim of this study is to geologically interpret aerogravity anomalies over the south-eastern part of the Niger Delta in order to map out the geologic structures in relation to hydrocarbon and mineral prospecting, and the specific objectives of this study are to determine the thickness of the sediments of the Southeastern Niger Delta Basin, basement topography, relationship between basement lineaments and sedimentation, and possible hydrocarbon elements.

2.0 Location

The area of study is located in the southeastern onshore part of the Tertiary Niger Delta Basin of Nigeria. It is part of Bayelsa, Rivers, Abia, Akwa Ibom, and Cross River States of Southern Nigeria. The area Figure 1lies between latitudes 4˚ 50' – 5˚ 50'N and longitudes 7˚ 00' – 9˚ 00'E. The topographic map (**Figure 2**) of the area indicates that elevations are in the range of 22.4 -187.5 m with the northwestern and eastern flanks having the highest elevations. The study area covers approximately 24,650 km².

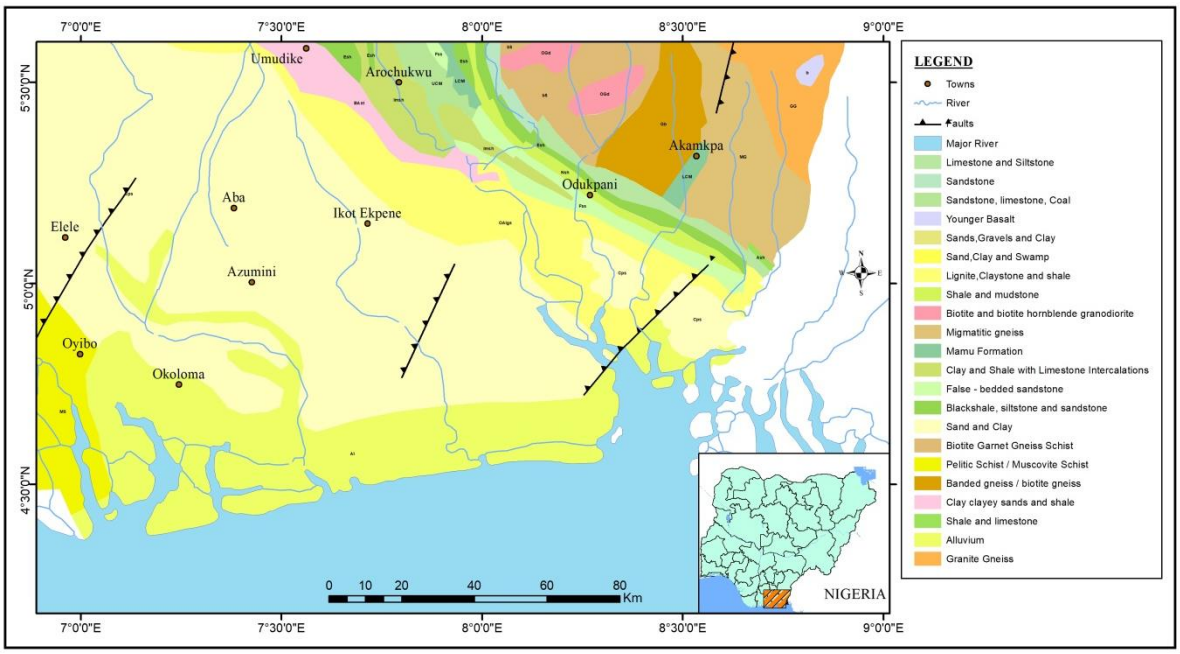

Figure 1: Location and Geologic map of the study area (Ekpo *et al*., 2024)

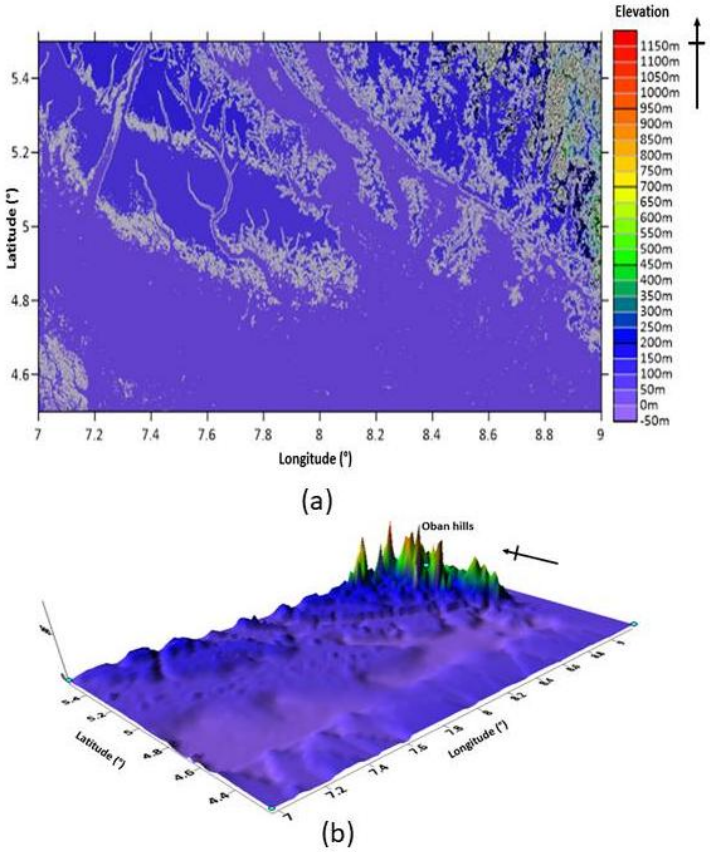

Figure 2: (a) 2D Topographic map of the study area. **(b)** 3D view of topographic map of the study area (USGS).

3.0 Materials

The aerogravity data acquired by the Nigerian Geological Survey Agency (NGSA) were used for the study. They include eight (8) gravity sheets of 321, 322, 323, 324, 329, 330, 331, and 332. The software programs used for data processing were Oasis Montaj version 7.0.1, Surfer (version 16.6), and ArcGIS (10.4).

3.1 Data Acquisition

The airborne gravity data was acquired and assembled by Fugro Airborne Surveys, Canada, between 2005 and 2010 for NGSA. These data were collected using a flux- adjusting surface data assimilation system with a flight-line space of 0.1 km, tie line space of 0.5 km, and terrain clearance ranging from 0.08 to0.1 km along 826,000 lines. The observed potential field data were of very high resolution when likened to the 1970 aero-geophysical data. These recent potential field data were noticed to be suited for mineral and petroleum investigations as well as geological mapping (Ekwok *et al*., 2020). The regional field in the Bouguer gravity data was subtracted by applying the tenth (10^{th}) International Gravity Standardization Net 1971(IGSN71) programs, by Fugro Airborne Surveys, Canada. The key benefit of the IGSN71 is the consistency they provide in potential field survey practice beginning from when the IGSN71 became available and generally accepted (Reeves et al., 1997, Ekwok *et al*., 2020). Fugro Airborne also carried out all other required potential field data treatments and reductions. The data used for this study were processed to be in the form of Bouguer gravity gridded data displayed as images in colour raster format **(**Figure 3).

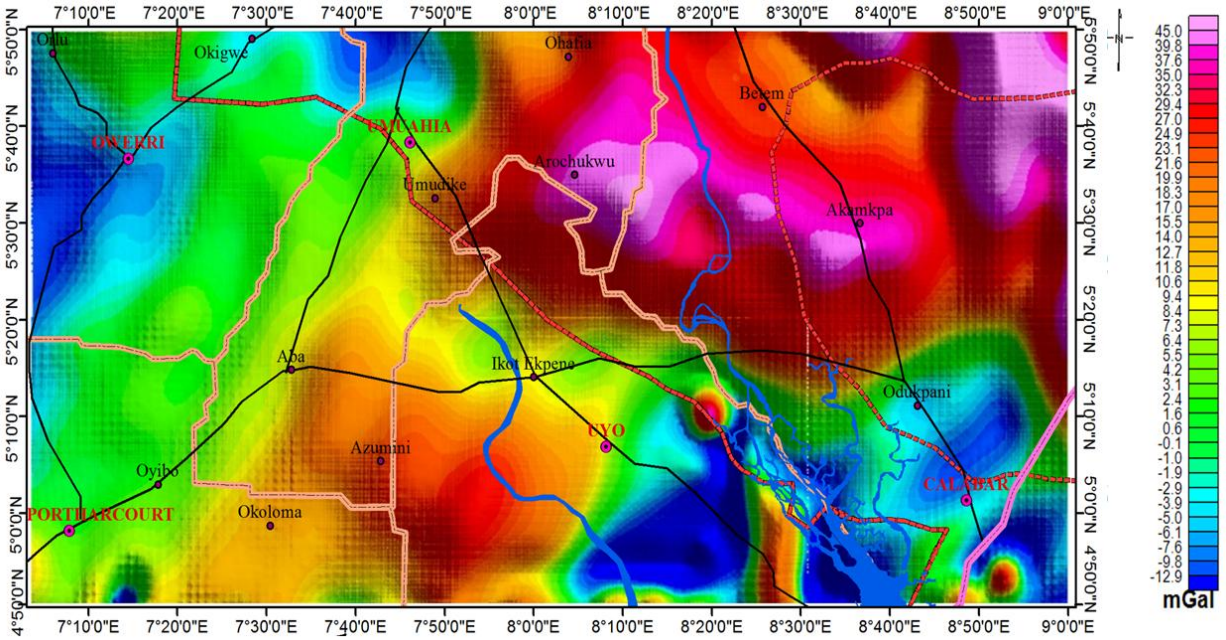

Fig. 3: Total Bouguer anomaly map of the study area

3.2 Methodology

The potential field data were incorporated into the World Geodetic System 84 (WGS 84) and Universal Transverse Mercator coordinate system at zone 32 of the northern Hemisphere (UTM 32N) in the Oasis Montaj program. The data directories were hosted in MAGMAP. Source parameter imaging, 3D Euler deconvolution, and GM-SYS tools, that created control files were employed in the different enhancements and modeling procedures

3.3 Filtering techniques

Qualitative and quantitative methods of data analysis were applied to the Bouguer gravity data. Qualitative data analysis and inter-pretation were applied first with the aid of Oasis Montaj software by digitizing the eight (8) Geosoft grid file format into X, Y and Z channels using the utility module of the gridding tools hosted in grid and map of the software package, and this was saved to a pre-created data base, which was created before the importation of the data sets. Filtering actions

like pre-spectrum analysis, which employs the fast furrier transform (FFT), were performed on each component of data before the regional-residual separation processes were done. This filtering action of regional, and residual separation using the X utility module was performed on the principal Z channel and thus the regional and residual channels were created by means of polynomial filtering of degree one (1) (see Figures 4and 5, respectively). This separation is based on the subtraction of the regional anomaly from the total Bouguer anomaly. The resultant effect is the residual map, which is the anomaly of interest. Filtering of the potential field data is an embodiment of procedures that consist of enhancing algorithms that carefully attenuate the anomalies from one set of geologic sources relative to anomalies due to other geologic sources (Milligan and Gunn, 1997). Typical potential field data filtering methods consisting of the first vertical derivative (Blakely and Simpson, 1986) and total horizontal and tilt angle derivatives (Hood and Teskey, 1972; 1989; Roest *et al*., 1992; Miller and Singh, 1994; Verduzco *et al*., 2004) were applied in this investigation from the residual map. To map the spatial distributions, and determine the different anomalous source depths, Euler deconvolution and radial power spectrum (Thurston and Smith 1997, Smith, *et al*., 1998) procedures were done. Likewise, the 2-D joint modeling was used to estimate depth to basement and delineate the basin framework as well as related intrusions and faults.

The aim of the filtering techniques is to separate the anomalies of different wavelengths from each other. That is, the separation of the local anomalies of shallow sources, which correspond to the anomalies of short wavelengths or high frequencies, from the regional anomalies of deep sources, which correspond to long wavelengths or low frequencies. In this work, the 2D filtering was carried out on the Bouguer map to identify the anomalies caused by geologic bodies and/or structural faulting, dislocations in the basement rocks at different depths. In the present study, the filtering technique used was the butter worth filter of the 1st filter number.

3.4 Radial power spectrum

This technique is used to estimate the depths of the shallow, intermediate, and deep geological structures. Several authors, such as Spector and Grant (1970), Bhattacharya (1994), Garcia and Ness (1994) and Muririzio ., (1998), explained the spectral analytical technique. It relies on the analysis of the gravity data using the Fourier transform on the spectral analysis map and its computer conjugate. It is a function of wavelengths in both the X and the Y directions. In this work, we applied the Fast Fourier transform (FFT) data to calculate the energy spectrum. The 2-D radially averaged power spectrum technique has been applied to determine the average depth level to the gravity source in the study area using the *Oasis Montaj* Program v.7.0.1.

3.5 Euler De-convolution

Euler deconvolution in one form or another has seen its application to gravity or magnetic data in geophysics for quite some time. Euler deconvolution is based on Euler's equation of homogeneity (Hood, 1965). The equation of homogeneity was specifically developed for magnetic data analysis. The application of the conventional Euler's de-convolution to both gravity data and magnetic gradients has been applied previously. However, most of these applications either used gravity gradients derived from vertical components in the measured gravity or were based on model simulation data (Zhang *et al*., 2000).

Thompson (1982) studied and applied the Euler deconvolution technique to potential fields' data and found out that the technique is helpful in speedy interpretation of potential field data in terms of geological structures and depth. Euler deconvolution aids the interpretation of gravity field, and involves the determination of

the location of the body causing anomalies based on analysis of gravity gradients, pulse gravity fields, and some constraints on the body geometry (Odek, *et al*., 2014).

The following is a review of the Euler's basic de-convolution concepts and also a derivation of Euler's de-convolution tensor for gravity tensor gradient. The technique applies the Euler equation of homogeneity.

$$(x - x_0)Tzy + (y - y_0)Tzy + (z - z_0)Tzz = N(Bz - Tz) \quad (3.1)$$

If we consider the vertical component of gravity anomaly of a body, Tz with homogeneous gravitational field, then the co-ordinatesx_0, y_0 and z_0 are the source body's unknown coordinates whose edges or center is being estimated and x, y, and z are the known coordinates of gravity and gradients of the observation point. The three value Tzx, Tzy, Tzz are therefore the gravity gradients $\frac{\partial T}{\partial x}, \frac{\partial T}{\partial y}$ and $\frac{\partial T}{\partial z}$measured along directions x, y and, z. N is thus the structural index, and Bz is the regional gravity value being estimated. Rewriting Equation (3.1), we get:

$$\mathrm{xTzx} + \mathrm{yTzy} + \mathrm{zTzz} + \mathrm{NTz} = x_0\mathrm{Tzx} + y_0\mathrm{Tzy} + z_0\mathrm{Tzz} + \mathrm{NBz} \quad (3.2)$$

In equation (3.2), there are four parameters that are unknown; x_0, $y_{0,}z_0$and B_z within a selected window of n number of data points available for solving the four unknown parameters. If n is greater than 4, these parameters can be estimated using other techniques such as Moore-Penrose inversion (Lawson and Hanson, 1974). The system uses a least squares method to solve Euler's equation simultaneously for each grid position within a window and then determines the anomaly position, depth, and base level for a specific gravity source. The obtained Euler deconvolution solution was applied to the Bouguer anomaly map with a specific structure index (SI). For the Bouguer gravity data, a structural index = 0, which indicates the presence of dyke, sill, step, and ribbon, was used. Maximum depth tolerance of 3 with a window size of 10 was applied. A maximum acceptable distance of 32000 m which is half the search window and a flying height of 100 m were used in the analysis.

3.6 Forward Modeling (Indirect Interpretation)

The parameters of the anomaly considered in modeling are; mass of the body M, depth from the surface to the centre of the body T, radius of the body R, and depth to the surface Z. Two dimensional forward modeling using the GM-SYS package of Oasis Montaj was used to define depth to the basement and delineate the basin frame of the area. The process involves computing the gravity responses, a creating hypothetical geologic model (Talwani *et. al*., 1959, Talwani and Heirtzler, 1964), and applying the algorithms described by Won and Bevis (1987). The data used for modeling were obtained along carefully drawn profiles on the residual gravity map.

4.0 Results

The regional gravity anomaly map (Figure 4) was produced through careful processing using the Butterworth with filter central wave number of 1900 of degree 2 and the prominent NE-SW (A, D), N-S (C), and NW-SE (B) trends persist. These reflect the deep extent of the subsurface structures causing these anomalies, which are interpreted to be of great depth and lateral extent. However, some smooth regional anomalies that appear not to be related to a subsurface structure can probably be associated with regional variation in the density of the rocks at great depth. A Bouguer gravity value that ranges from -7.3 mGal to 39.4 mGal is observed for the regional map. The eastern and the southeastern part of the study area, indicated by the blue colour, reveal area of low density materials. The blue colour is associated with subsurface material with low density,

which may be sedimentary in nature. This area might be said to be associated with hydrocarbon accumulation because of the closures in this area, which are associated with great depression or great sediment thickness.

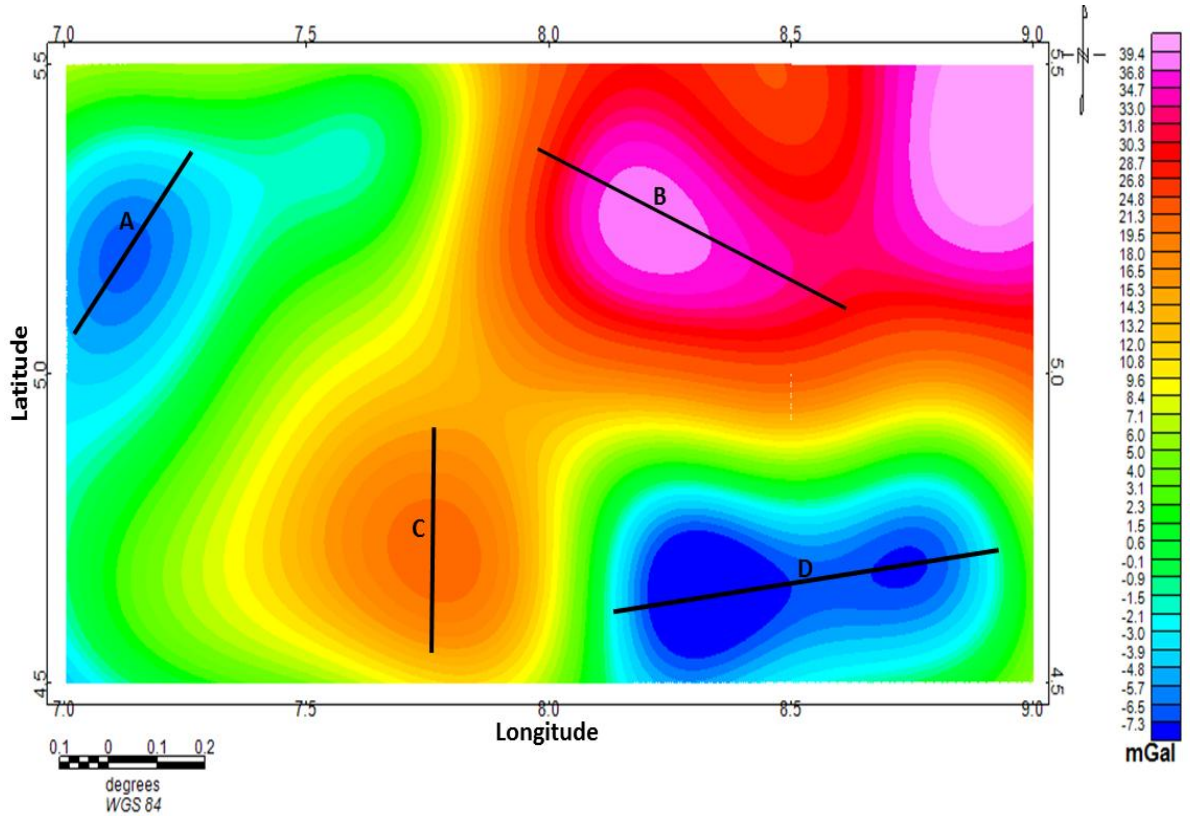

Figure 4: Regional gravity map of the study area showing the prominent trends

The residual Bouguer map (Figure 5**)** was produced with the butter worth gravity filtered with a filter central wave number of 3 of degree 8. The map reveals structural features indicated by linear, ellipsoidal, and other irregular shaped anomalies having their extension mostly in the N-S (F), NE-SW (A, D, E), and NW-SE (B, C) directions. These linear anomalies are mostly found at the edge of geologic structures of different shapes. The polarities of these anomalies are both positive and negative. Anomalies of different shapes and polarities are mostly found in the area, and these anomalies extend downward to the basement, and their trend is mainly NE-SW. These anomalies are mostly situated in the central, eastern, and north-western parts of the area. The negative polarities are associated with uplifting striking faults in the north, south, and western blocks, and they extend in the E-W and N-S directions. These faults have the main trends of NW-SE and N-direction. The residual map was divided into eight (8) blocks of D1 to D8 (Figure 6) and radial power spectrum analyses were carried out for each of the blocks. The radially averaged power spectrum (Figures 7a) shows the estimated average depth levels for the deep, intermediate, and shallow depth segments prevailing in the study area for each of the different blocks. The 2-D power spectrum plot (Figure. 7b) of depth against wave number of the gravity source bodies as it is directed to the basement surface and intra-basement sources, shows three depth ranges of deep, intermediate, and shallow sources as presented in Figure 8. This method of depth analysis using the radial power spectrum tends to provide a more consistent picture of depth in the two dimensions for digitized gravity data.

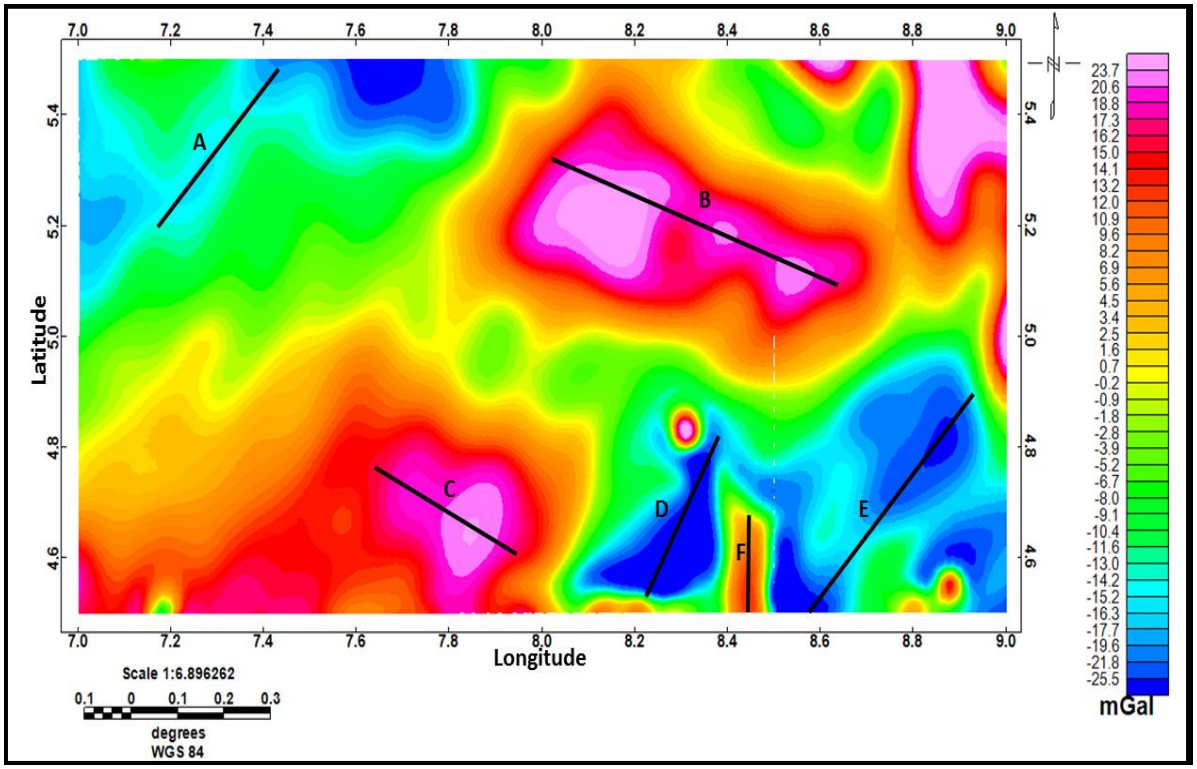

Figure 5: Residual gravity map of the study area showing the prominent trends

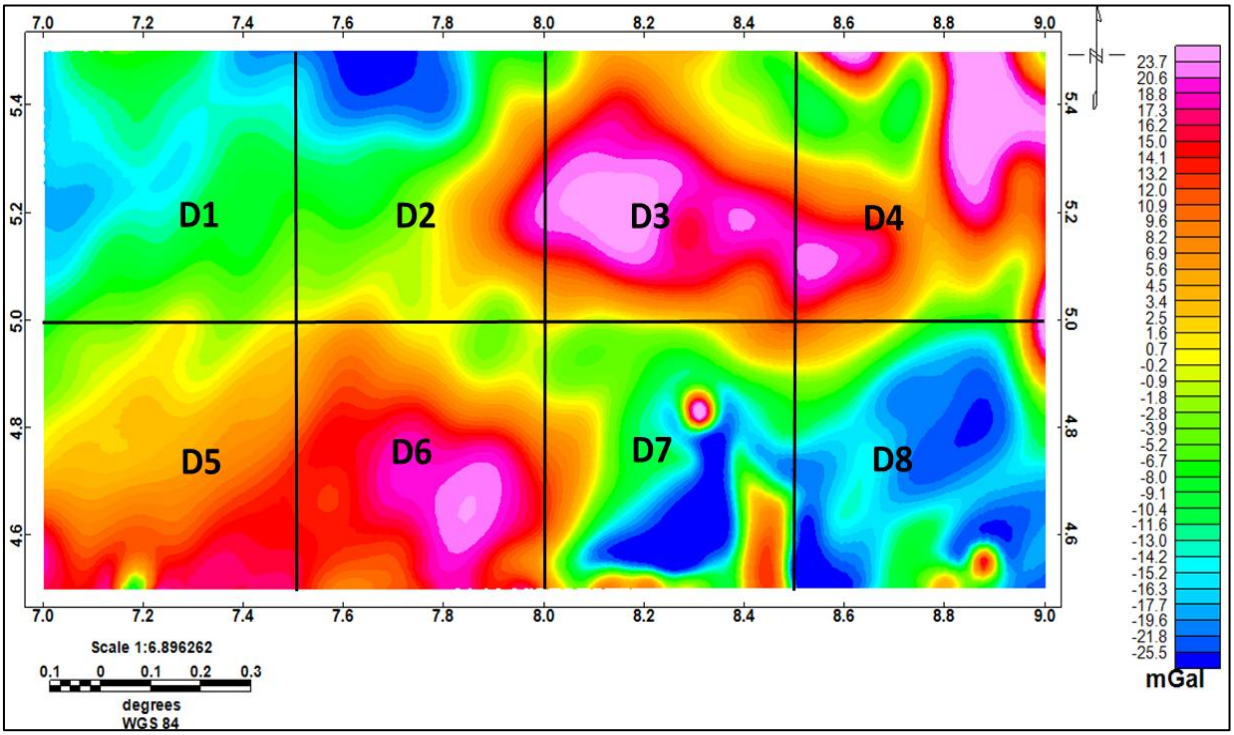

Figure 6: Residual gravity map divided into eight windows

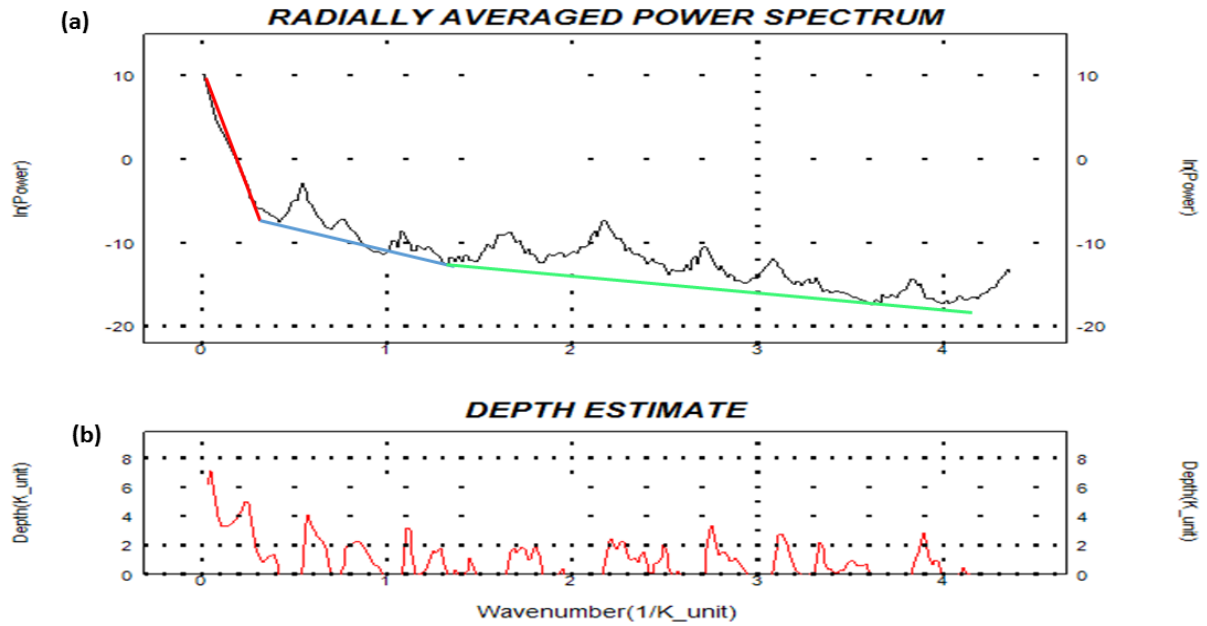

Figure 7a: (a) Radial average power spectral plot for block D1 (b) depth estimate plot for block D1

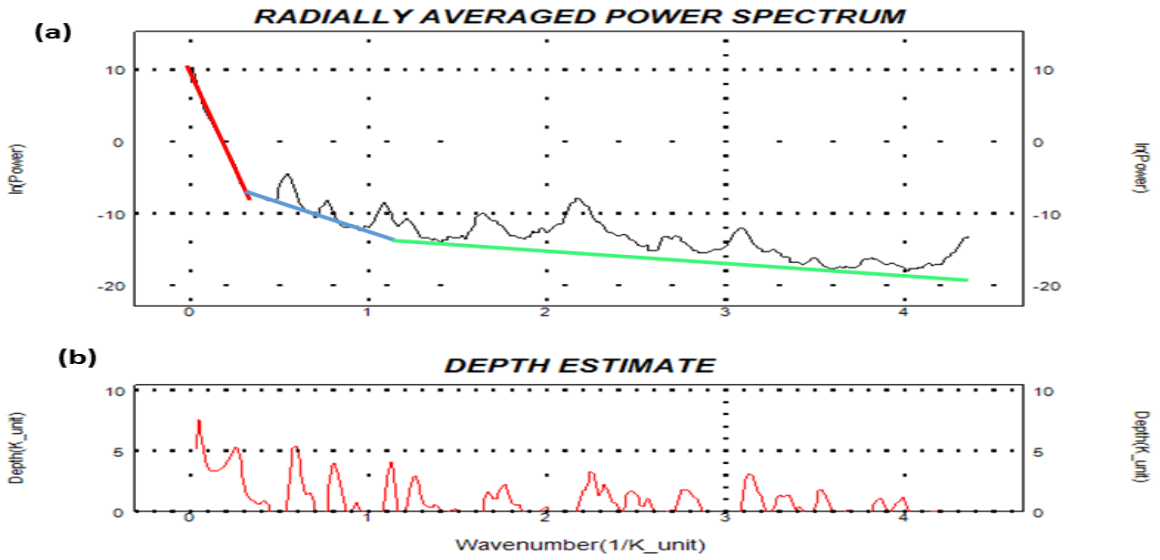

Figure 7b: (a) Radial average power spectral plot for block D2 (b) depth estimate plot for block D2

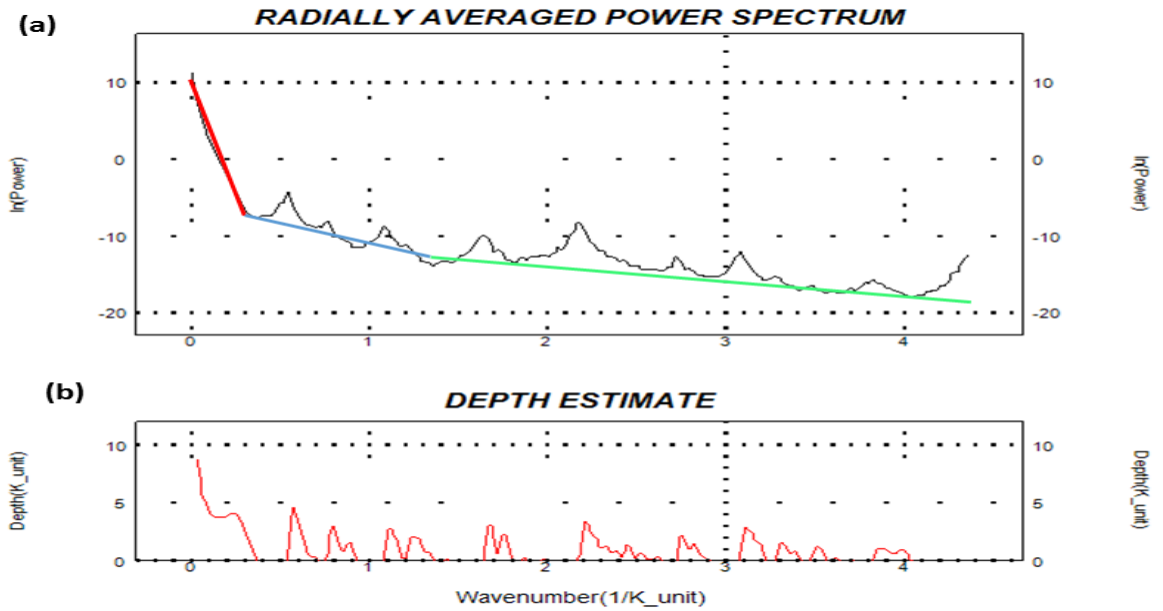

Figure 7c: (a) Radial average power spectral plot for block D3 (b) depth estimate plot for block D3

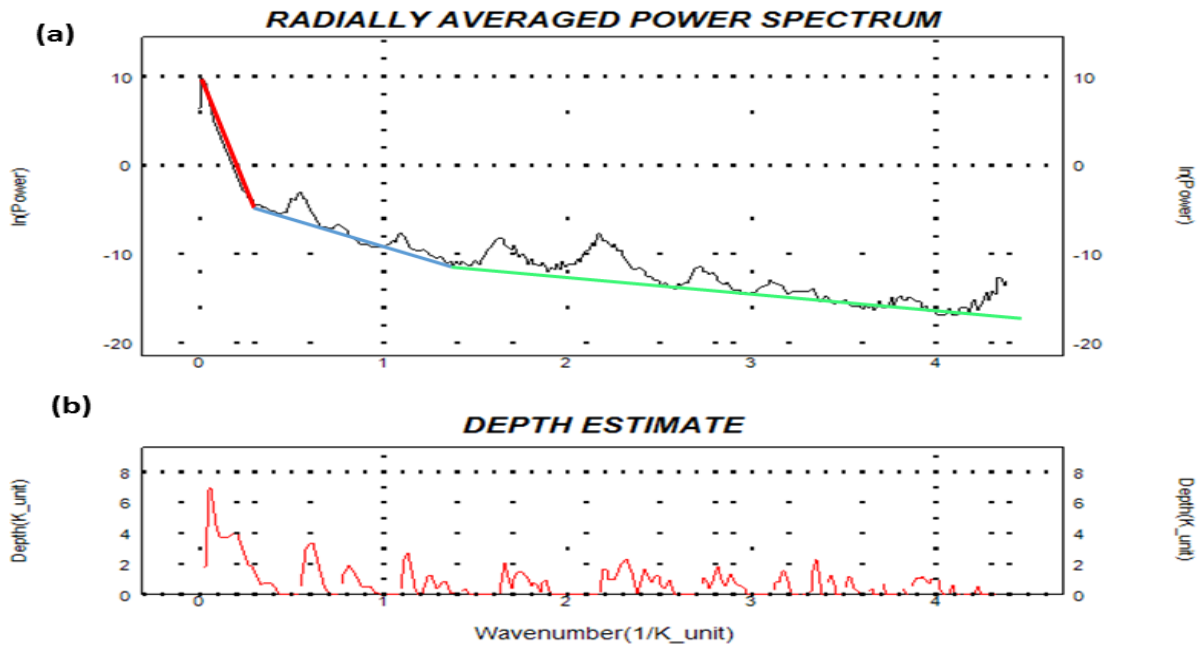

Figure 7d: (a) Radial average power spectral plot for block D4 (b) depth estimate plot for block D4

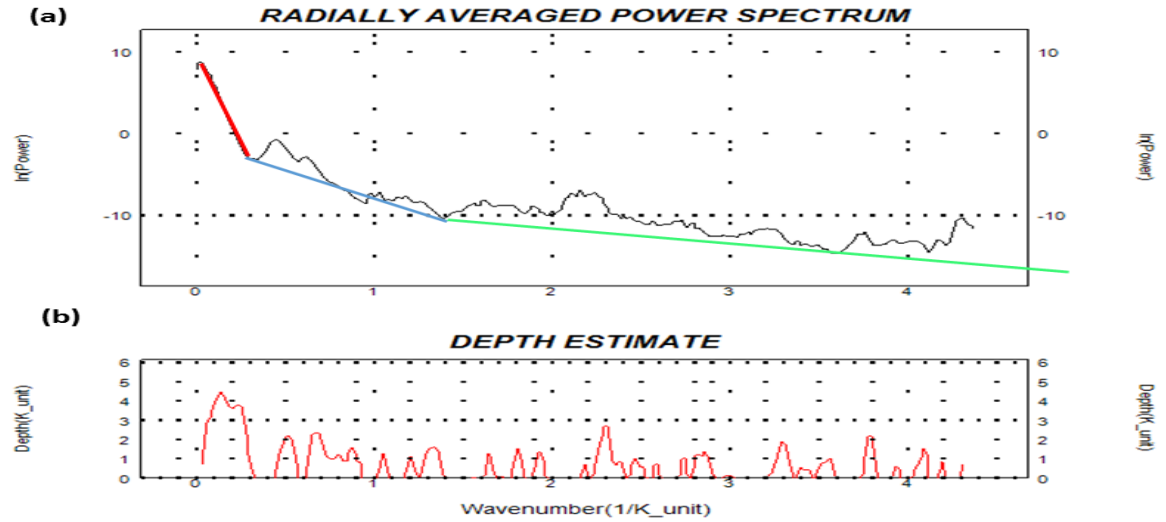

Figure 7e: (a) Radial average power spectral plot for block D5 (b) depth estimate plot for block D5

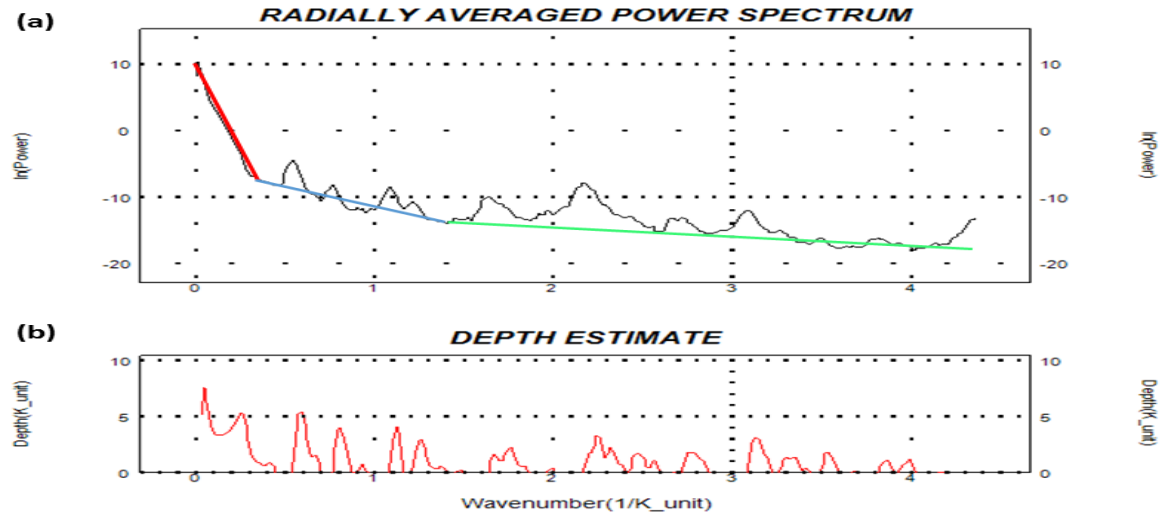

Figure 7f: (a) Radial average power spectral plot for block D6 (b) depth estimate plot for block D6

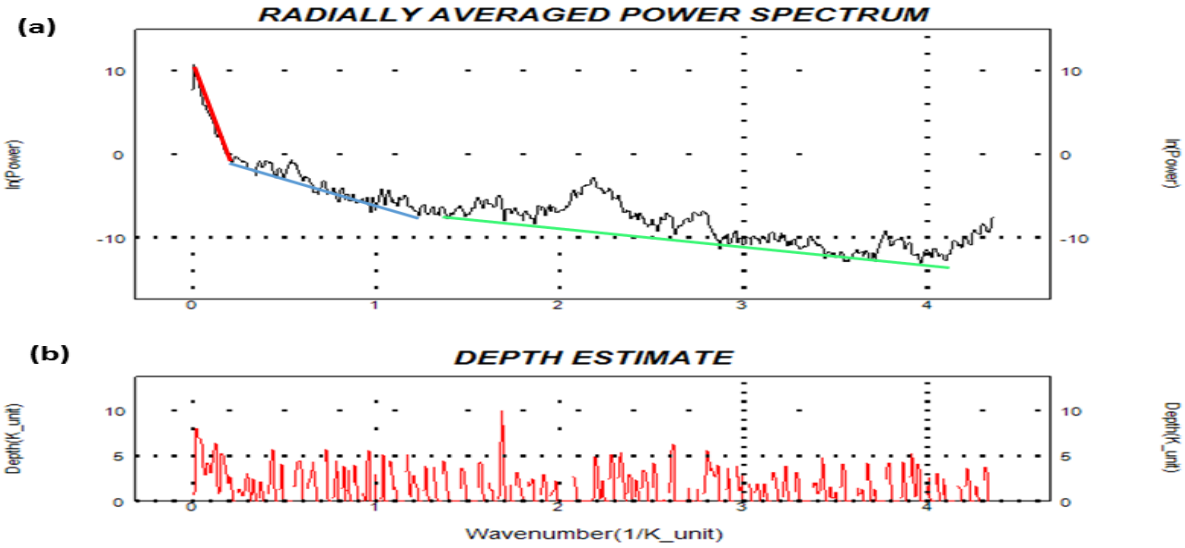

Figure 7g: (a) Radial average power spectral plot for block D7 (b) depth estimate plot for block D7

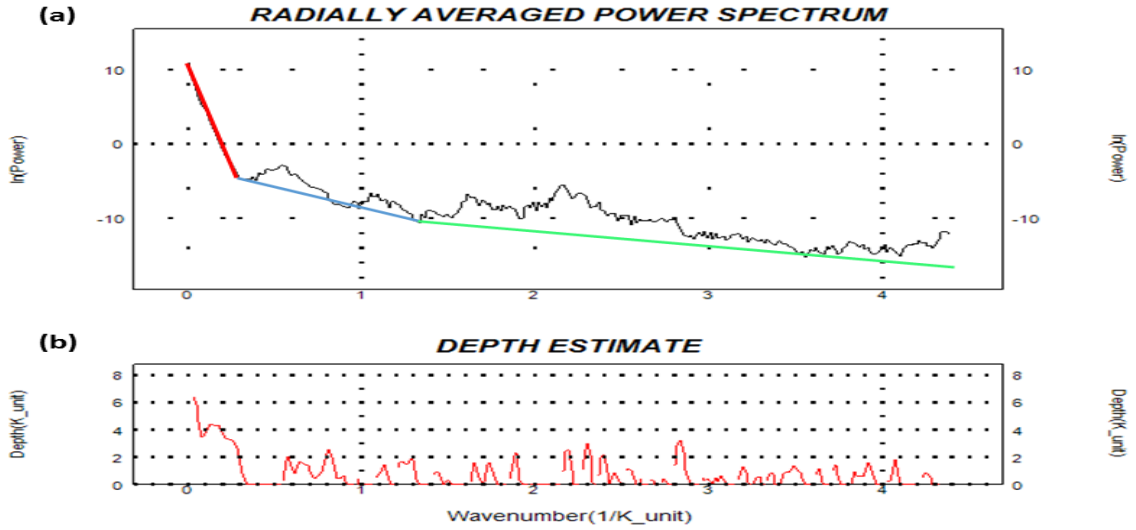

Figure 7h: (a) Radial average power spectral plot for block D8 (b) depth estimate plot for block D8

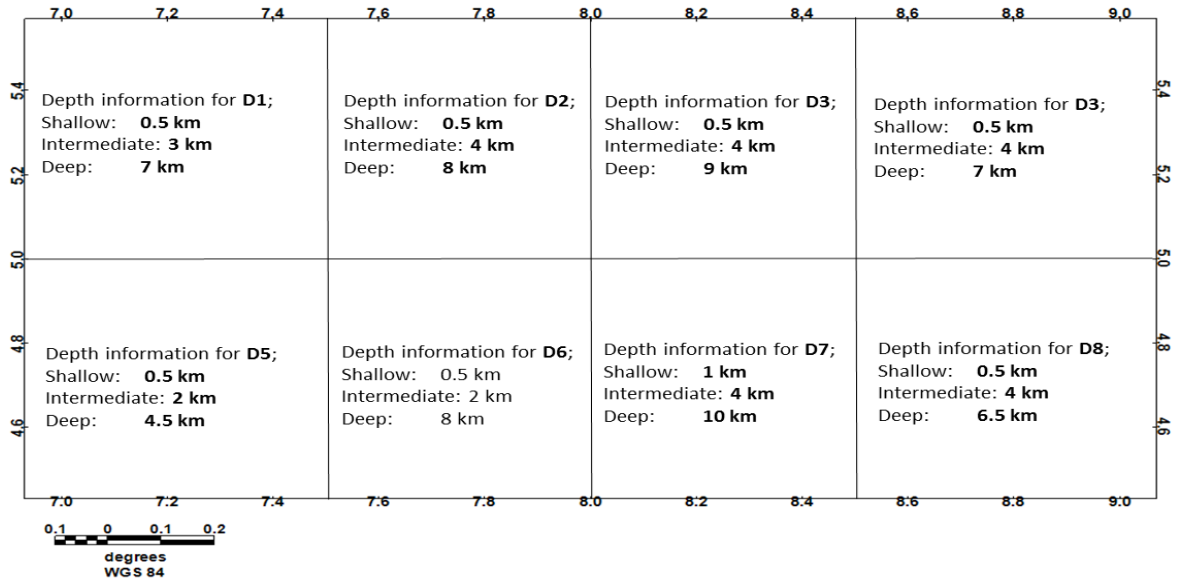

Figure 8: Radial power spectral depth information per window

The depth range obtained from Euler deconvolution analysis (Figure 9**)** of the study area ranges from a minimum depth value of less than 34.4 m to a maximum depth value of more than 8,228 m. The subsurface lineaments, which are fault structures, are mainly oriented in NNW-SSE, NE-SW and E-W directions. These trends are in alignment with the prevailing lineament structure of the Niger Delta. The white portions in the Euler deconvolution and 3D depth maps are the areas where the structural index cannot be estimated due to the small local wave number, which is automatically set to zero for the modeled independent wave number. The 3-D Euler deconvolution technique applied to the Bouguer data aids in detecting the locations and depth values of the different lineaments and it also aids mapping of the structural extent of the geologic body in the study area. The depth range from the Euler 3D depth solution analysis (Figure 10) indicates a range of minimum depth value of less than -111.4 m to maximum depth value of more than -7767.4 m. The surface/subsurface geologic structures as indicated from this map are oval and elongated. The lineaments, and fault structures trends in the NNW-SSE, NE-SW, and E-W, which are the trends of the prevailing lineament structure of the Niger Delta and the Benue Trough.

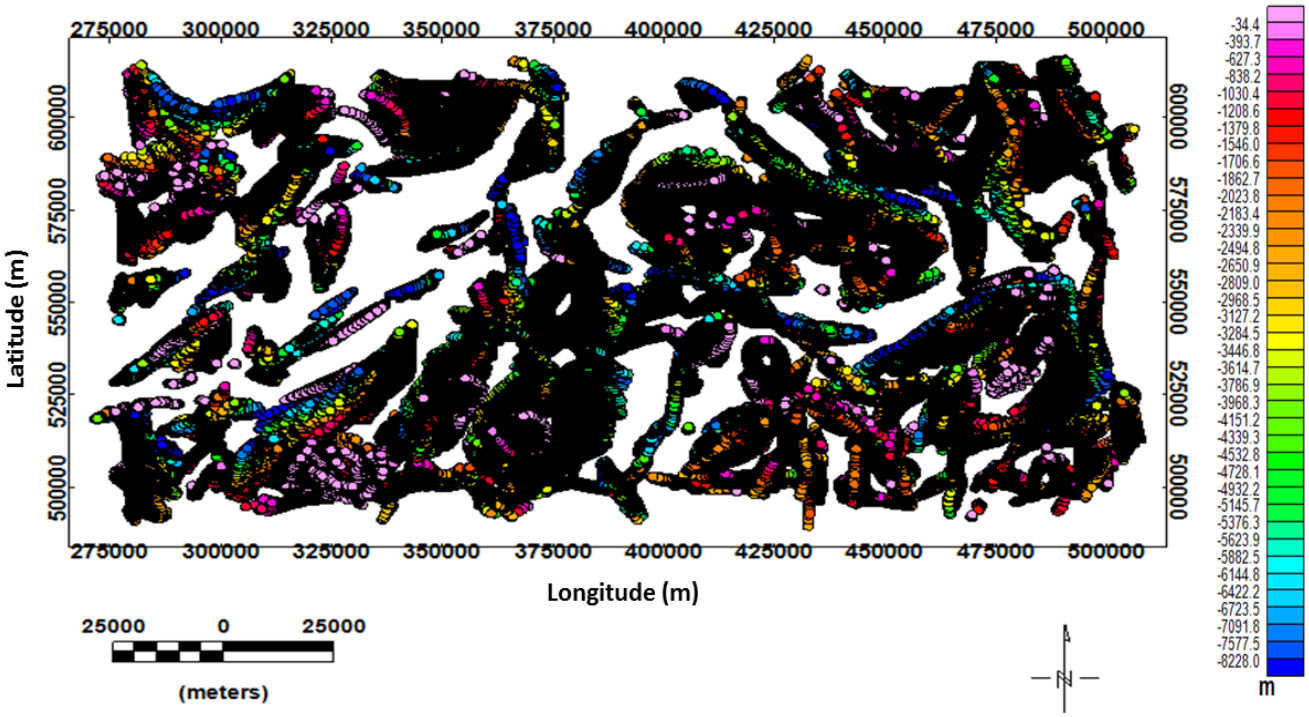

Figure 9: Euler deconvolution map showing depth to causative bodies and structural boundaries

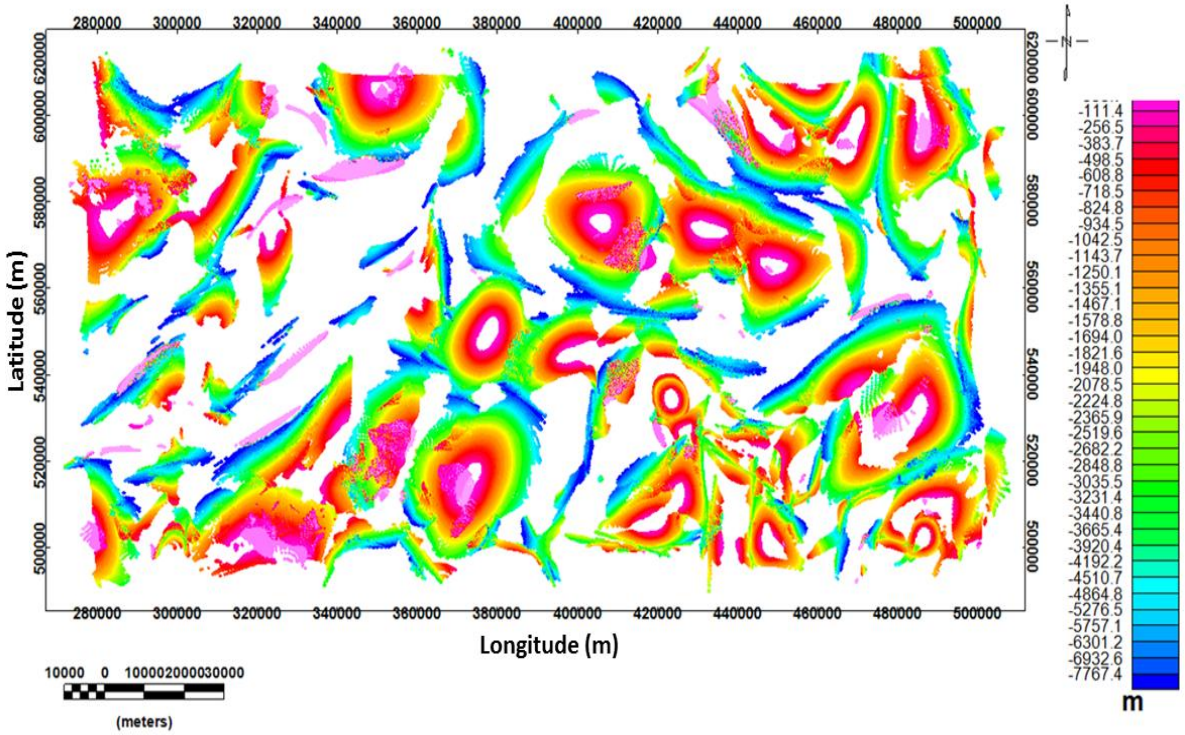

Figure 10: Euler 3D depth solution map showing depth distribution to causative bodies and their structural boundaries

A 2D forward modeling approach was employed on the Bouguer gravity data to characterize the subsurface geology and basement topography across various profiles in the study area. The analysis was based on the methods established by Talwani *et al*. (1959) and Talwani and Heirtzler (1964), with additional 2D formulations derived from Rasmussen and Pedersen (1979). The modeling was carried out using the GM-SYS toolkit within the Oasis Montaj program, and a profile length of ±30,000 km was adopted to minimize the edge effects typically encountered in such analyses. The interpreted 2D models were

generated from the gravity responses, reflecting subsurface geological structures derived from the SPI depth solution.

The selected profiles, shown in Figure 11, were strategically chosen to ensure comprehensive coverage of the study area and to intersect key geological features. The resulting models are presented in Figure 12.

Profile 1, illustrated in Figure 12a, extends west to east along 5.2°E of the map, covering an approximate distance of 220 km. The basement topography along this profile is generally undulating, reaching a maximum depth of about 7,500 m. A notable feature along this profile, marked as A, appears to be a major dyke intrusion, as suggested by the distinct uplift in the Bouguer gravity data at this location. Additionally, point B represents the deepest part of the basin along this profile.

Profile 2, shown in Figure 12b, also runs in a west-east direction, along 4.8°E of the map, spanning a similar length of approximately 220 km. The basement topography is characterized by undulations, with a maximum depth reaching 10,000 m. Noteworthy points along this profile include points C and D, which denote the deepest sections of the basin. Furthermore, point X exhibits a domal configuration, corroborating Olade's (1975) proposition that during the initial stages of the Niger Delta basin's evolution, mantle plume activity caused doming and subsequent rifting within the basin.

Profile 3, depicted in Figure 12c, follows a west-east trajectory along 4.6°E of the map and covers approximately 220 km. The basement along this profile is also undulating, with a maximum depth reaching 10,000 m. Points E and F indicate the deepest parts of the basin along this profile, further illustrating the variability in subsurface structure across the region. Profile 4, as shown in Figure 12d, runs southwest to northeast, from 7.6°E on the southwestern part of the map to 8.6°E on the northeastern side, covering a length of approximately 240 km. The basement topography here is similarly undulating, with a maximum depth of about 6,000 m. Points G and H mark the deepest parts of the basin along this profile, with point H aligning precisely with the location of the Calabar Flank. This profile reveals a series of horst and graben structures, with the Calabar Flank itself forming a graben at an approximate depth of 6,000 m.
Profile 5, represented in Figure 12e, extends from northwest to southeast, running along 5.28°N on the northwestern section of the map to 4.64°N on the southeastern end, and covers a distance of approximately 230 km. The basement topography along this profile also shows significant undulation, reaching a maximum depth of about 6,500 m. The deepest part of the basin along this profile is marked by point I.

The 2D forward modeling results reveal a complex subsurface, characterized by undulating basement topography and significant structural variations across all the profiles. Several key geological features are identified, including potential dyke intrusions, domal structures, and well-defined horst and graben formations. The findings provide a detailed depiction of the basement configuration, which shows significant lateral changes in depth and structure. The major dyke intrusion identified along Profile 1 suggests tectonic activities that may have contributed to localized deformation, while the domal feature along Profile 2 aligns with existing theories about mantle plume activity in the region.

Additionally, the presence of horst and graben structures, particularly evident along Profile 4, highlights the region's extensional tectonics and the processes that have shaped its geological history. The Calabar Flank, a prominent graben structure, points to substantial rifting activity, consistent with previous interpretations of the

area's tectonic evolution. These findings support the hypothesis that the subsurface geology has been significantly influenced by a combination of mantle dynamics, tectonic uplift, and extensional forces (Smith and Johnson, M. (2020).

Overall, the 2D forward modeling has provided new insights into the subsurface architecture of the study area, refining our understanding of the geological processes that have shaped the basin over time. The results emphasize the importance of integrating gravity data with other geophysical and geological information to develop a more comprehensive model of the subsurface. This study not only underscores the utility of Bouguer gravity data in mapping subsurface features but also lays the groundwork for future research that could further elucidate the tectonic and sedimentary evolution of the region. These findings may have broader implications for understanding the tectonic history of similar basins worldwide, contributing to both academic knowledge and practical applications in resource exploration.

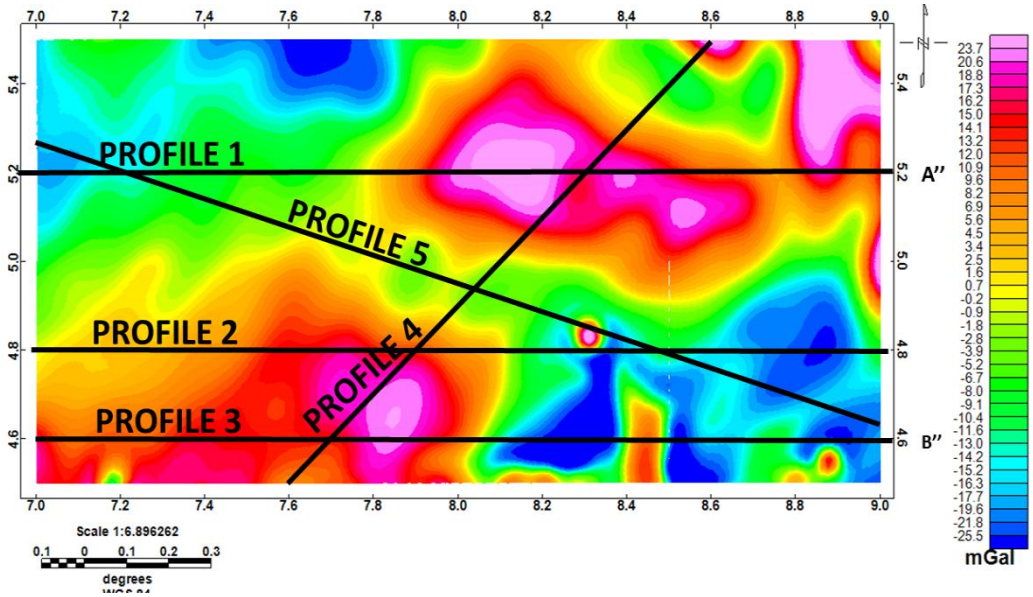

Figure 11: Residual map showing the Profile lines

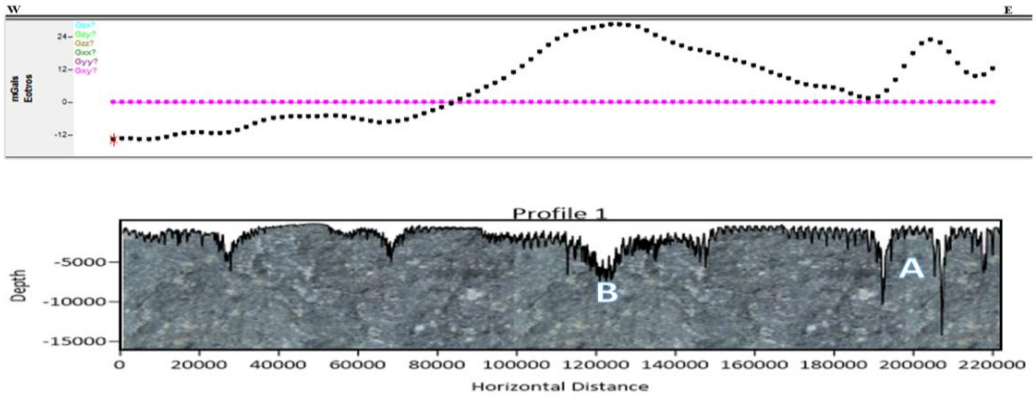

Figure 12a: 2D gravity model for Profile 1

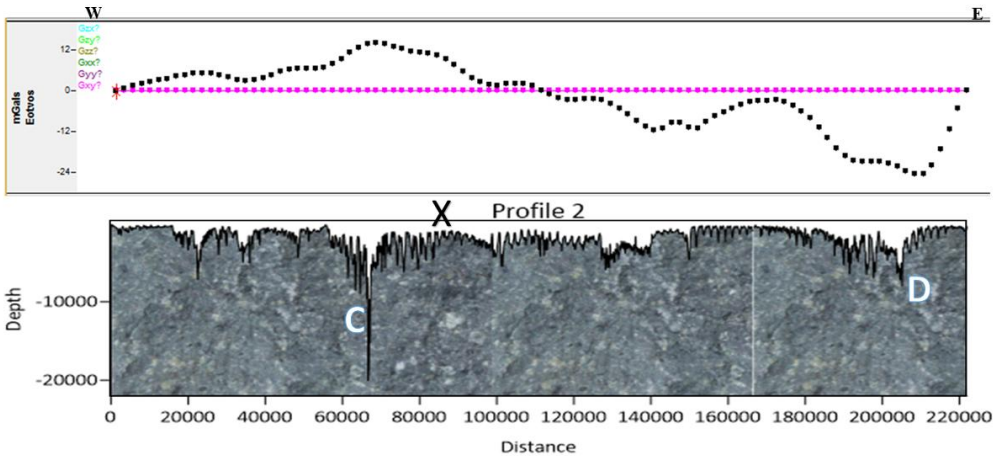

Figure 12b: 2D gravity model for Profile 2

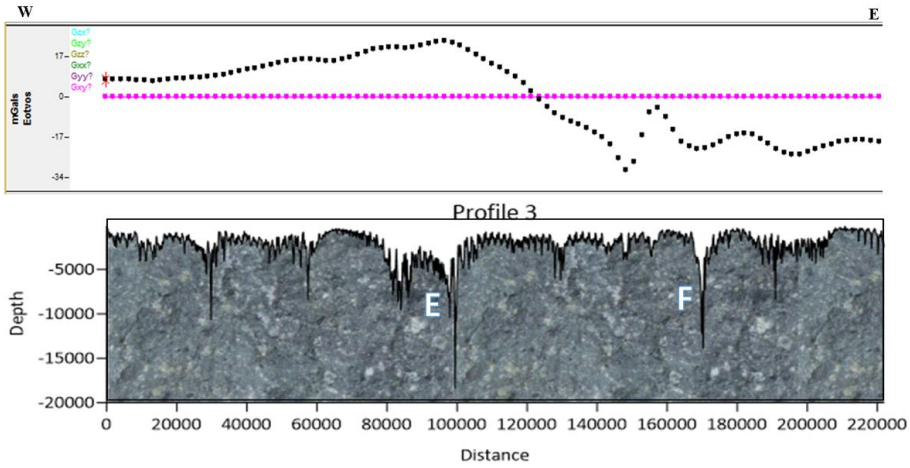

Figure 12c: 2D gravity model for Profile 3

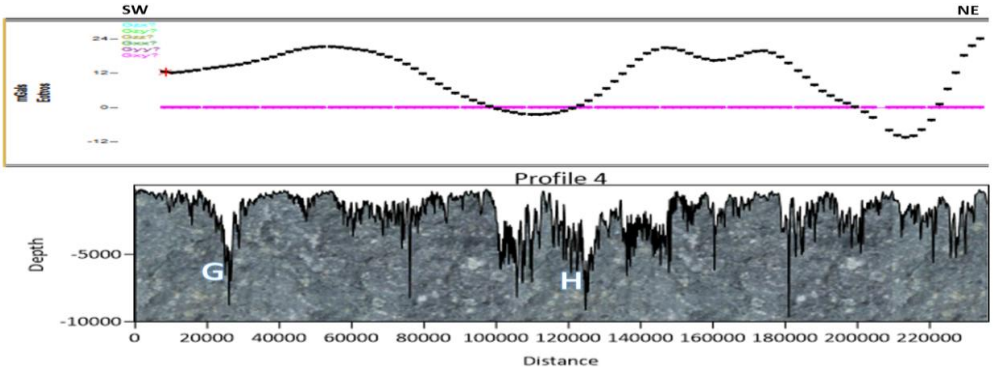

Figure 12d: 2D gravity model for Profile 4

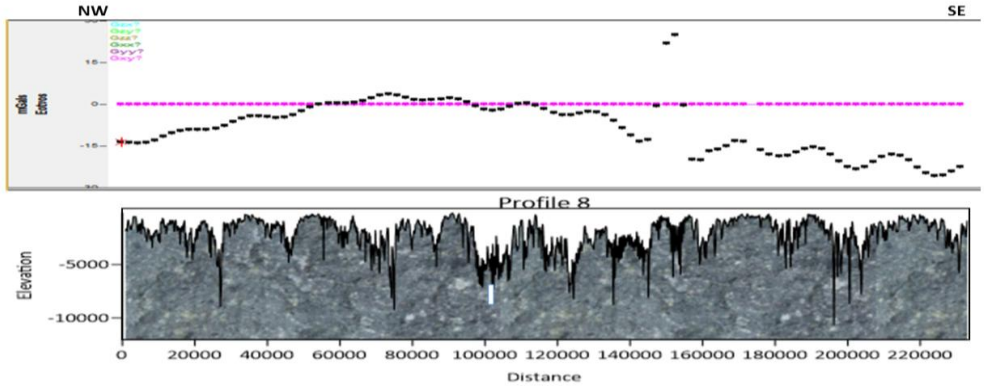

Figure 12e: 2D gravity model for Profile 5

5.0 Discussion of results

The Bouguer gravity high is found to be located at the outcrops of the Oban massif area of Odukpani and Akamkpa (Ekwok *et al*, 2021) and a little part of the Mamfe Embayment, and as a basic intrusion at Okwuiboku and at the boundary between Nigeria and Cameroon at the southeastern end of the study area. Moderately high gravity areas are found to be located within Degema area of Rivers State and Ini, Ikot Ekpene and Ukanafun in Akwa Ibom State (Figure 13).

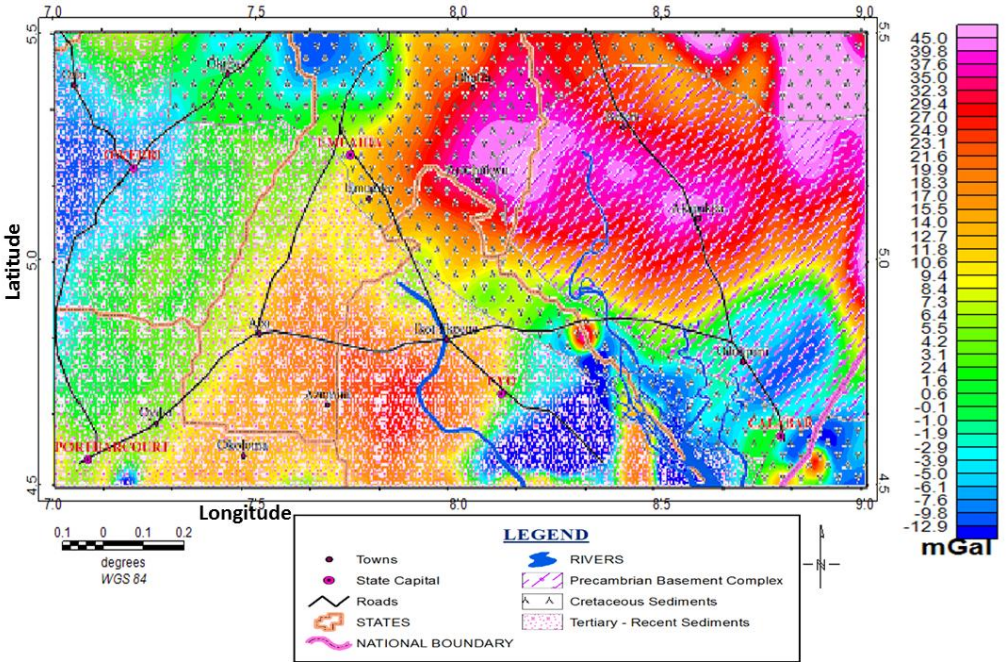

Figure 13: Overlay of Geologic map on Bouguer anomaly map showing density contrast over the study area

The analysis of the Bouguer gravity data revealed areas of low gravity values concentrated around Orlu, Owerri and its environs, as well as in Etinan, Calabar, and surrounding regions. The Bouguer anomaly map, represented using a range of color variations, depicts distinct lithological and structural features across the study area. These color differences delineate regions of low and high Bouguer gravity, with gravity values ranging from 12.0 mGal to 45.0 mGal. The color gradients on the map correspond to the combined gravitational effects of all subsurface rocks at specific points, thus highlighting horizontal variations in rock densities throughout the region.

The map reveals sub-structural trends in geological features that predominantly follow NE-SW, NW-SE, and N-S orientations. These structural alignments are believed to play a significant role in controlling drainage patterns and sediment deposition across the area. The intersection of the NE-SW and NW-SE trends emerges as a notable characteristic of the Niger Delta basin, discernible through visual inspection of the Bouguer gravity anomaly. Furthermore, areas of higher density sources were identified in the northeastern parts and within closures in the southeastern sections of the study area, while regions of lower density are observed in the northwestern and southeastern portions. A general southward decrease in rock density is evident over both the eastern and western halves of the map.

This trend of decreasing rock density aligns with findings by Khamies and El-Tarras (2010), who observed a similar southward reduction in density at the Quatara area of western Egypt. They suggested that such a decrease could indicate a deeper crust-mantle boundary in the southwestern region compared to the central and northern parts. In this context, a similar interpretation might be applicable here, where the gravity high observed in the northeastern part of the study area is associated with the Oban Massif. In this region, gravity values

range from 12.0 to 23.7 mGal (Figure 5), while gravity lows, with values between -25.5 and 1.6 mGal, correlate with significant depressions within the basin.

The Bouguer anomaly map (Figure 14) was contoured at a consistent interval of 1.8 mGal to facilitate a more detailed interpretation of the crustal structure in the study area. This contouring revealed strong positive gravity anomalies with trends primarily oriented in the NE-SW, NW-SE, and N-S directions. These trends appear irregular and variably spaced, likely reflecting significant variations in the basement's composition. The irregularity of these trends may result from a highly variable basement structure, while the observed spacing patterns suggest that the anomalies may originate from deeper geological sources (Emujakporue *et al.*, 2018). Additionally, the most prominent gravity high, trending NW-SE in the northeastern part of the study area, can be attributed to outcrops of the Oban Massif, which consists of granite, granodiorite, gneiss, and migmatite intrusions of Precambrian age.

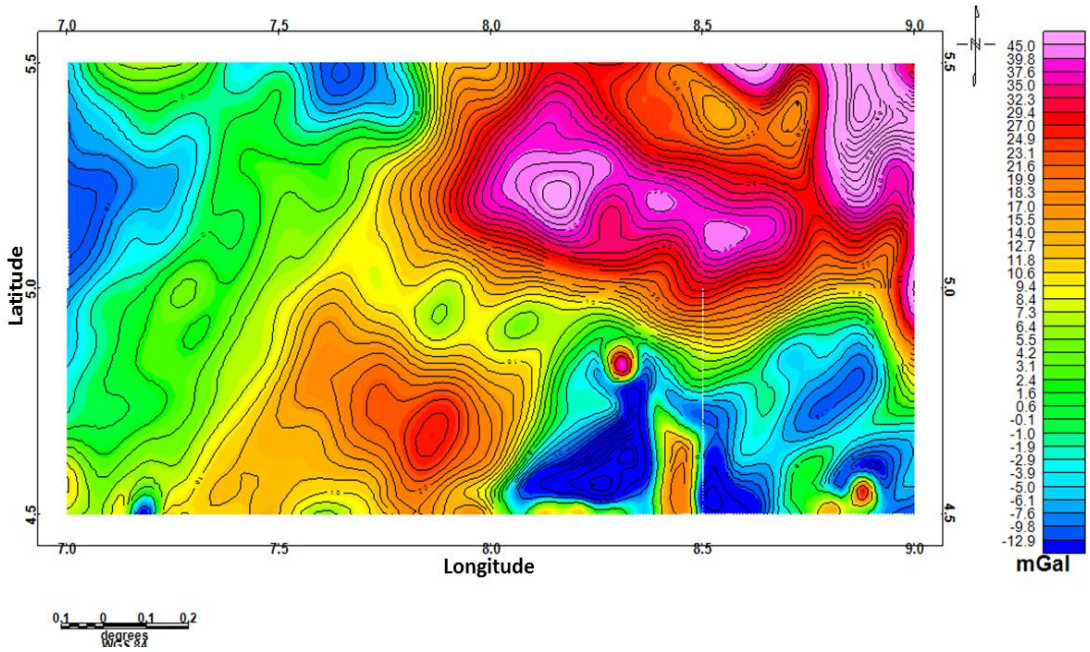

Figure 14: Contoured Bouguer Anomaly Map

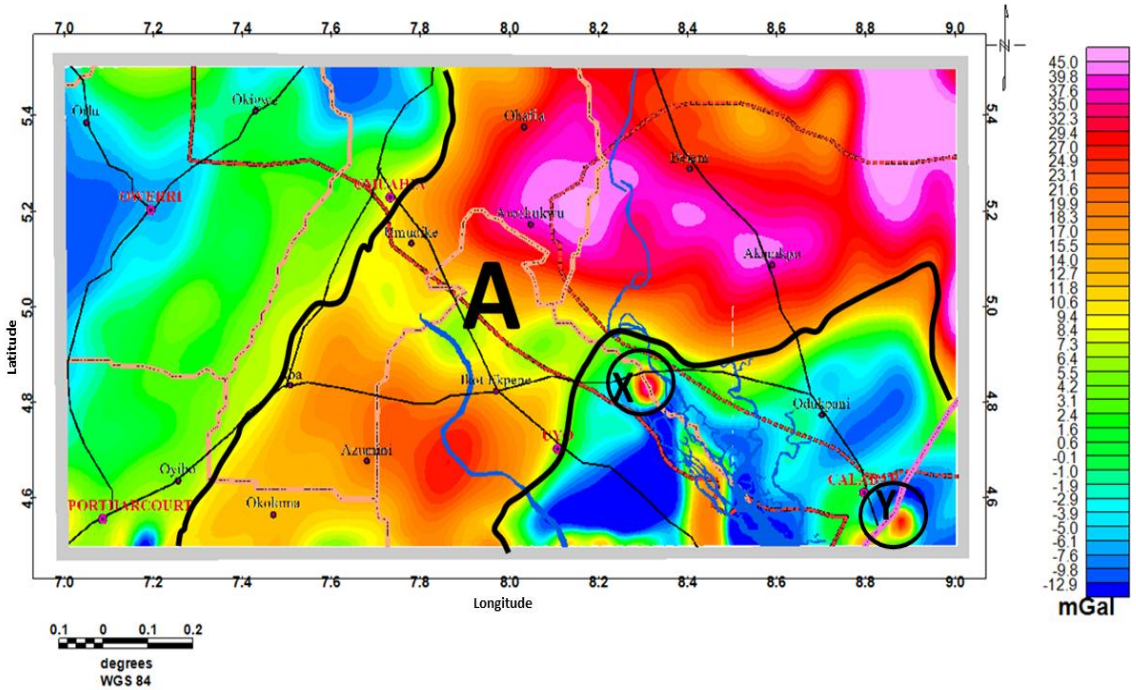

Figure 15: Bouguer Anomaly Map showing continuous basement

At the southeastern edge of the study area (Figure 15), two semicircular structures, marked as X and Y with a contour interval of 3.5 mGal, are interpreted as intrusions of a causative body vertically into the surrounding strata. The Bouguer anomaly map utilized in this study represents the summation of all gravitational effects from subsurface sources, encompassing both shallow and deep causative bodies, with the deeper, regional fields superimposed on the shallower, residual ones. The residual gravity map illustrates a range of anomalies, both linear and irregular, with gravity values ranging from -25.9 to -0.1 mGal in low-gravity regions, and from 0.2 to 23.0 mGal in high-gravity regions. Two distinct gravity lows are evident, indicated by blue and green hues, with the most significant low, shown in blue, located primarily in the southeastern part of the map around Calabar and its environs. The gradual shift from deep blue to lighter blue at the periphery of this region may be attributed to the weathering of granitic rock units.

High gravity anomalies associated with denser rock formations are predominantly found in the northeast, southeast, and southwest parts of the study area. The crystalline basement, characterized by high Bouguer anomaly values depicted in red to pink colors, extends from the southern part towards the Oban area in the northwest, with a discontinuity apparent between these regions on the regional map. The elevated Bouguer gravity observed around Aba, Ikot Ekpene, and adjacent areas may be interpreted as a block uplift, likely resulting from tectonic activity along plate boundaries and basin formation processes (Tuttle et al., 1978).

The similar orientation of the Precambrian basement underlying the Niger Delta basin and its outcrop at the Oban Massif suggests that these two regions could have been continuous before the formation of the Niger Delta basin. This similarity in basement rocks indicates possible down-faulting of the basement beneath the Niger Delta basin, providing further evidence for complex tectonic interactions that have shaped the geological evolution of the region.

6.0 Conclusion and Recommendation

6.1 Conclusion

The 2D forward modeling of Bouguer gravity data has provided valuable insights into the subsurface geology and basement topography of the study area, which are critical for hydrocarbon and mineral prospecting. The analysis reveals a complex subsurface structure characterized by significant variations in rock density, depth, and configuration, suggesting the presence of geological features conducive to hydrocarbon accumulation and mineral deposits.

Key features identified, such as potential dyke intrusions, domal structures, and well-defined horst and graben formations, indicate active tectonic processes that could create traps and reservoirs suitable for hydrocarbon storage. The major dyke intrusion along Profile 1 suggests tectonic activity that may have created fault-bounded traps or structural highs, while the domal configuration observed along Profile 2 aligns with mantle plume activity that could have induced thermal maturation of organic materials, enhancing hydrocarbon generation. Similarly, the horst and graben structures along Profile 4 reflect extensional tectonics that may have formed structural traps and stratigraphic pinch-outs, critical for hydrocarbon entrapment.

The Bouguer anomaly map, which delineates regions of low and high gravity values, also points to variations in rock densities that could signify different lithologies and structural settings. The higher gravity anomalies associated with dense rock formations, such as those in the Oban Massif, might indicate the presence of mineral deposits, including granitic and metamorphic rocks, which are often

associated with valuable minerals like gold, tin, and rare earth elements. The observed general southward decrease in rock density may also suggest changes in crustal composition, indicating areas where hydrocarbon-bearing sediments could be more abundant or where mineral-rich zones are present.

Overall, the study underscores the utility of Bouguer gravity data in identifying key geological features that are critical for both hydrocarbon and mineral exploration. Integrating these findings with additional geophysical and geological data could enhance the identification of prospective areas, guiding further exploration efforts.

6.2 Recommendations

Target Structural Traps and Fault-Bounded Features: Areas identified with structural traps, such as domal uplifts and faulted blocks, should be prioritized for hydrocarbon exploration. The dyke intrusion along Profile 1 and the domal features along Profile 2 could represent significant hydrocarbon reservoirs or traps. Detailed seismic surveys and exploration drilling should be conducted in these areas to validate the presence of hydrocarbons.

The horst and graben structures observed along Profile 4 indicate extensional regimes that may have created conditions favorable for hydrocarbon accumulation. These structures could form traps where hydrocarbons generated from deeper sources have migrated and accumulated. Further geophysical studies, including 3D seismic reflection surveys, are recommended to delineate these features in detail and assess their hydrocarbon potential.

High gravity anomalies, particularly in the northeast and southeast regions associated with dense rock formations such as the Oban Massif, should be investigated for their mineral prospectivity. These areas may contain economically valuable minerals like gold, tin, and rare earth elements often associated with granitic intrusions, gneiss, and migmatite. Ground surveys, geochemical sampling, and targeted drilling should be employed to evaluate these zones for mineral exploration.

Implementing advanced geophysical techniques, such as high-resolution aero-magnetic surveys and 3D forward modeling, can help in accurately mapping the extent and geometry of subsurface structures. This approach would provide a more precise characterization of potential hydrocarbon traps and mineral-rich zones, thereby reducing exploration risks and costs.

By leveraging these findings, exploration companies can strategically target areas with the highest potential for hydrocarbon and mineral deposits, thereby optimizing exploration investments and improving the chances of successful discovery.

Declarations

Conflict of interest: The author declare that they have no known competing financial interests or personal relationships that could have appeared to influence the work reported in this paper.

HUMAN ANIMAL RIGHTS:

This article does not contain studies with human or animal subject.

References

Amigun, J. O. and Ako, B. D. (2009). Rock Density-A tool for mineral prospection: A case Study of Ajabonoke Iron Ore Deposit, Okene, Southwestern Nigeria. The Pacific Journal of Science and Technology. pp. 733-741.

Bhattacharya, J., (1994). Cretaceous Dunvegan formation of the Western Canada Sedimentary Basin. In: Mossop, G.D., Shetsen, I. (comp.), Geological Atlas of

the Western Canada Sedimentary Basin, Canadian Society of Petroleum Geologists and Alberta Research Council, p. 365–374.

Blakely, R.J. & Simpson, R.W., (1986) Approximating edges of source bodies from magnetic or gravity anomalies, *Geophysics*, 51, 1494-1498.

Ekpo, A. E., Bassey, N. E., George, N. J. (2024). Aero-gravity data analysis for delineating possible channels of mineralizations migration through lineament.A case study of Southeastern Niger Delta, Nigeria.AKSU Annels of Sustainable Development 2(1), 139-168, 2024.https://doi.org/10.60787/AASD-v2i1-35

Ekwok, S. E., Akpan, A. E. & Kudamnya, E. A., (2020). Exploratory mapping of structures controlling mineralization in Southeast Nigeria using high resolution airborne magnetic data. J*ournal of African Earth Sciences*, 162, 103700.

Ekwok, S. E., Akpan, A. E. & Ebong, E. D. (2021). Assessment of crustal structures by gravity and magnetic methods in the Calabar Flank and adjoining areas of Southeastern Nigeria - a case study of the obudu massif. *Arabian Journal of Geo-sciences*, 14**,** 308. .https://doi.org/-10.1007/s12517-021-06696-1.

Emujakporue, G., Ofoha, C. C., Kiani, I. (2018). Investigation into the basement morphology and tectonic lineament using aeromagnetic anomalies of Parts of Sokoto Basin, North Western, Nigeria. Egyptian Journal of Petroleum, Volume 27, Issue 4, Pages 671-681, ISSN 1110-0621, https://doi.org/10-.1016/j.ejpe.2017.10.003.

Ezekiel, J. C, Onu, N. N, Akaolisa C. Z, Opara A. I. (2013). Preliminary Interpretation of gravity mapping over the Njaba sub-basin of Southeastern Nigeria. An implication to petroleum potential. Journal Geology and Mining Research, 5(3):75-87.

Garcia, J. G. and Ness, G. E., (1994). Inversion of the power spectrum from magnetic anomalies. *Geophysics* 59, 391–400.

Gram, C., Hanssen, P., Myrlund, E.A., and Hood P., (1965). Gradient measurements in aeromagnetic surveying. Geophysics, Volume 30, Issue 5, Pages: 705-932ISSN (print):0016-8033ISSN (online):1942-2156

Hood, P. J. & Teskey, D. J., (1989). Aeromagnetic gradiometer program of the geological survey of Canada. *Geophysics*, 54(8), 1012-1022.

Khamies, A. & El-Tarras, M. (2010).Surface and subsurface structures of Kalabsha area, southern Egypt, from remote sensing, aeromagnetic and gravity data. World Pumps, 13.43-52. 10.1016/j.ejrs.-2010.07.006.

Lawson, C. L., Hanson, R. J. (1974). Solving Least Squares Problems. Prentice-Hall, Englewood Cliffs.

Milligan, P. & Gunn, P., (1997). Enhancement and presentation of airborne geophysical data. *AGSO Journal of Australian Geology and Geophysics*, 17 (2), 63–75.

Murphy, B. S. (2007). Airborne Geophysics and the Indian scenario. Journal of Industrial *Geophysics*, 11(1): 1-28.

Obiora, D. N, Ossai, M. N, Okeke, F. N, Oha, A. I. (2016). Interpretation of airborne geophysical data of Nsukka area, Southerneastern Nigeria.Journal of the

Geological Society of India. 88:654-667.

Odek, A., Otieno, A. B., Ambusso, W. J. and Githiri, J. G., (2012). 2d-Euler deconvolution and forward modeling of gravity data of homa-hills geothermal prospect, kenya. Journal of Agriculture, Science and Technology, Vol. 15(1)

Okiwelu, A. A, ofrey-Kulo, O, Ude, I. A. (2013). Interpretation of regional magnetic data offshore Niger Delta reveals relationship between deep basement architecture and hydrocarbon target. Earth Science Research, 2(1):13-32.

Okpoli, C. C. and Akingboye, A. S. (2019). Application of high-resolution gravity data for litho-structural and depth characterisation around Igabi area, Northwestern Nigeria, NRIAG. Journal of Astronomy and Geophysics, 8:1, 231-241, DOI: -10.1080/20909977.2019.1689629

Rasmussen, R. and Pedersen, L.B. (1979) End Corrections in Potential Field Modeling. Geophysical Prospecting, 27, 749-760. https://doi.org-/10.1111/-j.1365-2478.1979.tb00994.x

Reeves, C., Reford, S., & Millingan, P., (1997). Airborne geophysics: old methods, new images. In: Gubins, A. (Ed.), Proceedings of the Fourth Decennial *International Conference on Mineral Exploration*, 13 – 30

Roest, W. R., Verhoef, J., Pilkington, M., (1992). Magnetic interpretation using the 3-D analytic signal. *Geophysics*, 57(1), 116-125.

Smith, J., and Johnson, M. (2020). *Tectonic Evolution and Geodynamics of the Niger Delta Basin: Insights from Gravity Data Analysis*. Journal of Geophysical Research, 125(8), 1582-1595. Doi: 10.1029/jgrb215825.

Smith, R. S., Thurston, J. B., Dai, Ting-fan, and MacLeod, L.N. (1998). The Improved Source Parameter Imaging Method: Geophysical Prospecting, Vol. 46, pp. 141-151.

Spector, A., Grant, F. S., (1970). Statistical models for interpreting aeromagnetic data. *Geophysic*s, 35, 293–302.

Talwani, M., Heirtzler, J. R., (1964).Computation of magnetic anomalies caused by two dimensional structures of arbitrary shape. In: Computers in the mineral industries. Part 1: Stanford University Publications, Geological Sciences, 9, 464–480.

Talwani, M., Worzel, J. L. and Landisman, M., (1959). Rapid gravity computations for 2 dimensional bodies with application to the Mendocino submarine fracture zone. Journal of Geophysical Research, 64, 49-59.

Thompson, D. T. (1982). EULDPH-A New Technique for Making Computer Estimates from Magnetic Data. *Geophysics*, 47:31-37.

Thurston, J. B. & Smith, R. S., (1997). Automatic conversion of magnetic data to depth, dip, and susceptibility contrast using SPITM method. Geophysics, 62, 807-813.

Tuttle, M., Charpentier, R., and Brownfield, M., (2015). "The Niger Delta Petroleum System: Niger Delta Province, Nigeria, Cameroon, and Equatorial Guinea, Africa". United States Geologic Survey.

United States Geologic Survey. Retrieved 6 March 2015.

Verduzco, B., Fairhead, J. D. Green, C. M. and MacKenzie, C., (2004).New insights into magnetic derivatives for structural mapping. The Leading Edge, 23, 116–119.

Won, I. J. and Bevis, M. (1987). Computing the Gravitational Magnetic Anomalies Due to a Polygon: Algorithm and FORTRAN Subroutines. *Geophysics*, 52, 232-238. https://doi.org/10.1190-/1.1442298

Zhang C, Mushayandebvu, M. F., Reid A. B., Fairhead J. D. and Odegard M. E. (2000).Euler De-convolution of Gravity Tensor Gradient Data. Geophysics, 65:512-520.